Proceedings of the 3rd International Symposium on Uncertainty Quantification and Stochastic Modeling
D.A. Rade; A. M. G. Lima (Editors), ABCM, Maresias, SP, Brazil, February 15-19, 2016

Robust Optimization of the Aeroelastic Behavior of Tow Steered Composite Plates

Thiago A. M. Guimarães[1], Domingos A. Rade[2], and Aldemir A. Cavalini Jr.[1]

[1] Federal University of Uberlândia, School of Mechanical Engineering, Uberlândia, MG, Brazil

[2] Technological Institute of Aeronautics, Division of Mechanical Engineering, São José dos Campos, SP, Brazil

Abstract: The use of tow steered laminate composite plates, in which the fibers follow pre-specified paths has shown to be capable of improving the aeroelastic behavior of plate-like structures using only discrete choices of fiber orientation $(0/90/45/-45)^0$*. Accounting for the potential benefits of this design strategy and the inevitable presence of uncertainties in actual manufacturing process, the study reported in this paper proposes a robust optimization methodology to increase the aeroelastic stability margin, accounting for uncertainties affecting tow steering and fiber placement angles. The strategy is applied to an idealized model of a cantilever wing, consisting of a small symmetric composite plate containing six plies, which has already been used in a number of previously reported works, for various purposes. The aeroelastic model used to evaluate flutter and divergence instability results from the combination of a structural model based on the Rayleigh-Ritz approach and a quasi-steady aerodynamic model based on the strip theory with the inclusion of the term of unsteadiness in pitch velocity.Moreover, the deterministic optimization is performedby using the algorithm of differential evolution, and the robust optimization combines deterministic analysis with a Monte Carlo Simulation and Latin-Hypercube Sampling.*

Keywords: aeroelasticity, composite materials, tow steering, robust optimization, aeroelastic tailoring

NOMENCLATURE

X-29 = Forward-sweep wing aircraft
VAT = variable angle tow
AFP = automatic fiber placement
ATL = automatic tape laying
CLT = Classical Lamination Theory
CTS = Continuous Tow Shearing
MCS = Monte Carlo Simulation
PCE = Polinomial Chaos Expansion
DOE = Design of Experiments
C1 = [0 -45 45]s laminate
C2 = [-45 45 45]s laminate
Q_{11} to Q_{66} = Engineering Constants for ortotropic Material
κ = out of plane curvatures
M = out of plane momments
D = Bending torsion stiffness terms
T0= start tow steering angle
T1= end tow steering angle
U_1 to U_4 = Material Invariants
ζ_9 to ζ_{12} = Lamination Parameters
s=semi-span
c=chord
f^{eff}= global mean objective function
a_w = wing lift curve slope
e = eccentricity factor
W = work done by the aerodynamic lift and moment
A = Mass matrix
E = Stiffness matrix
B = Aerodynamic damping matrix
C = Aerodynamic stiffness matrix

INTRODUCTION

The extensive use of composite materials in aerospace structures became a reality due to largely recognized benefits such as high specific stiffness and strength as compared to traditional metallic materials. Much effort has been devoted recently to the optimization of composite structures aiming at increasing, as much as possible, their performance. In this sense, the design strategy consisting in tailoring the plies in different orientations is not a recent practice. As a matter of fact, (Munk, 1949) reports the orientation of wood fibers to allow favorable deformation of propeller blades. In the 1980s a large amount of scientific works were produced followed by the development of the experimental forward-sweep wing flight demonstrator aircraft, the X-29, whose maiden flight occurred in 1984 and the divergence problem was solved in part by arranging bending and torsion deformation coupling in composite wing (Shirk *et al.*, 1986).

Despite the existence of a number of academic studies that confirm the potential of the use of composite aeroelastic tailoring methods, the industry has not extensively explored their benefits in the design of commercial composite aircraft wings (Stodieck *et al.*, 2014) yet. This is partially due to the difficult to certify composite laminates with stacking sequence different from traditional discrete choices (0/90/45/45). Nevertheless, the emergence of new manufacturing process, such as continuous tow shearing (CTS), which enables to minimize process-induced defects (Kim *et al.*, 2014) and improve the structural benefits, makes these procedures attractive to new developments. It is worth mentioning the use of automated tape laying (ATL) in the production of the Boeing 787 and A350XWB commercial aircrafts, which provided increased productivity (Lukaszewicz *et al.*, 2012).

Moreover, as a result of the improvement of the automated fiber placement (AFP) technique tow steering has been developed to allow laminates to be constructed with variable angle tow (VAT) plies in which the fibers are placed following curvilinear paths, in such way that is possible to achieve additional structural design improvements (Parnas *et al.*, 2003). From the structural standpoint there is a considerable amount of work that demonstrated both analytically and experimentally the benefits in terms of buckling and post-buckling behavior of VAT plates (Lopes *et al.* (2008), Gürdal *et al.* (2008), Kuo and Shiau (2009). Other studies are devoted to the vibrational (Akhavan and Ribeiro, 2011) and aeroelastic (Stodieck *et al.* (2013), Stanford *et al.* (2014)) behavior of VAT flat plates.

Following the trend observed in various disciplines, the influence of parameter uncertainties on the aeroelastic stability of composite structures have been investigated using various techniques such as Monte Carlo Simulation (MCS), Polynomial Chaos Expansion (PCE), surrogate modeling, stochastic collocation (Scarth *et al.*, 2015). In this context, this paper investigates an efficient robust optimization procedure for the design of tow-steered composite rectangular plates subjected to uncertainty in the tow steering angles. The aeroelastic analysis is performed for a simple dynamic model of the composite structure derived by using the Rayleigh-Ritz approach, in combination with a quasi-steady aerodynamic model based on the strip theory. Moreover, the deterministic optimization is performed by using the algorithm of differential evolution, and the robust optimization combines deterministic analysis with Monte Carlo Simulation and Latin-Hypercube Sampling.

THEORETICAL MODEL

Fig. 1 depicts a top view of a VAT ply, in which the curves indicate the trajectories of the fibers. In the following sections, the structural, aerodynamic and aeroelastic models for VAT laminated composite plates are derived.

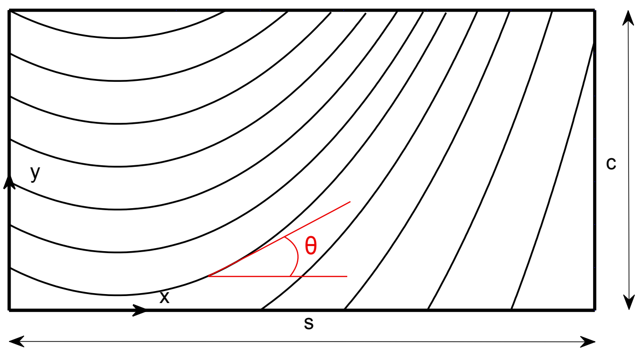

Figure 1: Fiber placement trajectory for a variable stiffness plate

Structural Model

The structural dynamic model was obtained by using the classical Rayleigh-Ritz approach, which is based on the use of the Lagrange Equations of motion in association with the following approximation for the transverse displacement field for the plate, which is compatible with the boundary conditions of cantilever plates:

$$w(x, y, t) = \sum_{m_0}^{m_{max}} \sum_{n_0}^{n_{max}} q_{mn}(t) \left(\frac{x}{s}\right)^m \left(\frac{y}{c} - 0.5\right)^n \tag{1}$$

Being n_{max}=1 to satisfy the criteria of chordwise rigidy to approximate behavior of a common wing, and $m_0 = 2$, $n_0 = 0$ to satisfy the boundary conditions at the clamped edge and $n_{max} = 8$ evaluated from convergence analysis.

The Rayleigh-Ritz approach requires the formulation of the kinetic and strain energies, as follows.

Assuming the underlying hypotheses of the Kirchhoff theory, which is adequate for thin plates, the kinetic energy is expressed as:

$$T(t) = \frac{1}{2} \int \int \rho \dot{w}^2 dx dy \tag{2}$$

where ρ is the surface density of the material (kg/m^2).

Under the same hypotheses, the strain energy is given by:

$$U(t) = \frac{1}{2} \int_0^c \int_0^s \mathbf{S}^T \mathbf{D} \mathbf{S} dx dy \tag{3}$$

where:

$$\mathbf{S}(x,y,t) = \left[-\frac{\partial^2 w}{\partial x^2} \quad -\frac{\partial^2 w}{\partial y^2} \quad -2\frac{\partial^2 w}{\partial x \partial y} \right] \tag{4}$$

and (**D**) is the the bending-torsion stiffness (**D**) matrix, which depends on the elastic constants and fiber angle within the ply. In the case of VAT plates, this matrix must be computed accounting for the fact that this angle varies over the plate as shown in 1.

For the case considered herein, it can be shown that matrix (**D**) is given by:

$$\mathbf{D}(x) = \begin{bmatrix} D_{11}(x,y) & D_{12}(x,y) & D_{16}(x,y) \\ D_{12}(x,y) & D_{22}(x,y) & D_{26}(x,y) \\ D_{16}(x,y) & D_{26}(x,y) & D_{66}(x,y) \end{bmatrix} \tag{5}$$

Being the steering, the first important definition, expressed by:

$$\theta = \theta_i + \frac{T1 - T0}{s} x + T0 \tag{6}$$

where θ_i is the ply angle, $T0$ the initial tow steering angle in the root, and $T1$ the final tow steering angle in the plate tip.

Then, it is show the engineering constants for an ortotropic material.

$$Q_{11} = \frac{E_1}{1-\nu_{12}\nu_{21}}, \qquad Q_{22} = \frac{E_2}{1-\nu_{12}\nu_{21}}, \qquad Q_{12} = \frac{nu_{12}E_2}{1-\nu_{12}\nu_{21}}, \qquad Q_{66} = G_{12} \tag{7}$$

Being ν_{21}:

$$\nu_{21} = \frac{E_2 \nu_{12}}{E_1} \tag{8}$$

The terms form matrix (**D**) were expressed as function of material invariants (U_1 to U_4), originally formulated by (Jones, 1998).

$$U_1 = \frac{3Q_{11} + 3Q_{22} + 2Q_{12} + 4Q_{66}}{8}, \qquad U_2 = \frac{Q_{11} - Q_{22}}{2}, \tag{9}$$

$$U_3 = \frac{Q_{11} + Q_{22} - 2Q_{12} - 4Q_{66}}{8}, \qquad U_4 = \frac{Q_{11} + Q_{22} + 6Q_{12} - 4Q_{66}}{8} \tag{10}$$

And lamination parameters (ζ_9 to ζ_{12}) proposed by (Tsai, 1980).

$$\begin{bmatrix} \zeta_9(x,y) \\ \zeta_{10}(x,y) \\ \zeta_{11}(x,y) \\ \zeta_{12}(x,y) \end{bmatrix} = \frac{3}{2} \int_{-1}^{1} \begin{bmatrix} cos2\theta(x,y) \\ cos4\theta(x,y) \\ sin2\theta(x,y) \\ sin4\theta(x,y) \end{bmatrix} u^2 du \tag{11}$$

Where $u = 2z/h$ being z the distance from mid-plane. And finally, the matrix terms of matrix **D** is:

$$\mathbf{D} = \begin{bmatrix} D_{11}(x,y) \\ D_{12}(x,y) \\ D_{22}(x,y) \\ D_{16}(x,y) \\ D_{26}(x,y) \\ D_{66}(x,y) \end{bmatrix} = \frac{h^3}{12} \begin{bmatrix} 1 & \zeta_9(x,y) & \zeta_{10}(x,y) & 0 \\ 0 & 0 & -\zeta_{10}(x,y) & 1 \\ 1 & -\zeta_9(x,y) & \zeta_{10}(x,y) & 0 \\ 0 & \zeta_{11}(x,y)/2 & \zeta_{12}(x,y) & 0 \\ 0 & \zeta_{11}(x,y)/2 & -\zeta_{12}(x,y) & 0 \\ 0.5 & 0 & \zeta_{10}(x,y) & -0.5 \end{bmatrix} \begin{bmatrix} U_1(x,y) \\ U_2(x,y) \\ U_3(x,y) \\ U_4(x,y) \end{bmatrix} \tag{12}$$

Aerodynamic Model

The assumed aerodynamic model is based in the combination of quasi-steady aerodynamic forces from strip theory, enhanced with the inclusion of an unsteady pitch velocity term ($M_{\dot{\theta}}$=-1.2) as suggested in (Hancock, 1995). According to this model, the infinitesimal increments of the lift force and moment on a strip in the span-wise direction are given by:

$$dL = \frac{1}{2} \rho_{air} V^2 c a_w \left(\frac{\dot{w}}{V} + \theta \right) dx \tag{13}$$

$$dM = \frac{1}{2}\rho_{air} V^2 c^2 \left[e a_w \left(\frac{\dot{w}}{V} + \theta \right) + M_{\dot{\theta}} \left(\frac{\dot{\theta} c}{4V} \right) \right] dx \tag{14}$$

Being, V and ρ_{air} the airflow velocity and air density respectively. Moreover, a_w is the effective wing lift curve slope, which is assumed to be a function of the position of the strip along the span according to:

$$a_w = 2\pi \left[1 - \left(\frac{x}{s} \right)^3 \right] \tag{15}$$

and the load eccentricity factor e is defined as the distance between the aerodynamic center, assumed to be at one fouth of the chord and the position of the shear axis that is assumed to be at half of the chord. Thus,

$$e = \frac{(y_{ref} - y_{ac})}{c} = \frac{1}{4} \tag{16}$$

Stodieck *et al.* (2013) show the validation of the modified strip theory at low speeds by comparison with the standard Doublet Lattice implement in NASTRAN®.

Therefore, the aerodynamic loads are introduced in the Rayleigh-Ritz scheme through the computation of the virtual work, as follows:

$$\delta W = \int_0^s \left(-dL \delta w + dM \delta\theta \right) dx \tag{17}$$

Aeroelastic Model

The aeroelastic model, resulting from the interaction between the plate and the surrounding air flow, is obtained by using Lagrange Equations, expressed in the following form:

$$-\frac{\partial L}{\partial \mathbf{q}} + \frac{d}{dt} \left(\frac{\partial L}{\partial \dot{\mathbf{q}}} \right) = \mathbf{Q} \tag{18}$$

where $L = T - U$ is the Lagrangean function, $\mathbf{q} = [w \quad \theta]^T$ is the vector of generalized coordinates and $\mathbf{Q} = [Q_w \quad Q_\theta]^T$ is the vector of generalized forces.

Associating equations 2, 3 and 17 to Eq.18, the aeroelastic equations of motion are obtainded as follows:

$$\mathbf{A}\ddot{\mathbf{q}} + \rho V \mathbf{B}\dot{\mathbf{q}} + \left(\rho V^2 \mathbf{C} + \mathbf{E} \right) \mathbf{q} = 0 \tag{19}$$

or, in the state space form:

$$\left\{ \begin{array}{c} \dot{\mathbf{q}} \\ \ddot{\mathbf{q}} \end{array} \right\} = \left[\begin{array}{cc} \mathbf{0} & \mathbf{I} \\ -\mathbf{A}^{-1}(\rho V^2 \mathbf{C} + \mathbf{E}) & -\rho V \mathbf{A}^{-1}\mathbf{B} \end{array} \right] \left\{ \begin{array}{c} \mathbf{q} \\ \dot{\mathbf{q}} \end{array} \right\} \tag{20}$$

where **A** is the mass matrix, **E** the stiffness matrix and **B C** account for the aerodynamic contributions to damping and stiffness, respectively.

The aeroelastic stability analysis is performed by solving the eigenvalue problem associated to the matrix equation 20, for increasing values of the flow speed V. By inspecting the complex eigenvalues expressed as:

$$\lambda = -\zeta_n \omega_n \pm j\omega_n \sqrt{1 - \zeta_n^2} \qquad \text{n=1,2...}(n_{max} - n_0)(m_{max} - m_0) \tag{21}$$

where ω_n and ζ_n are the undamped natural frequencies and and modal damping factors, respectively, two types of aeroelastic instability can be found: the first is the case of static instability named *divergence*. It occurs when system becomes non-oscillating ($\omega_n = 0$) and the modal damping factor becomes negative ($\zeta_n < 0$); the second is the case of the dynamic instability known as *flutter*. It emerges when dynamic system is oscillating ($\omega_n > 0$) but the modal damping factor becomes negative ($\zeta_n < 0$)

The flutter and divergence air speeds are found solving Eq. 21. The instability by definition occurs when any one of damping ratios ζ_n becomes negative.

Fib. 2 shows typical evolutions of the natural frequencies and damping factors of an aeroelastic system comprising for three vibration modes. As can be seen, divergence is reached at lower flow speed, as compared to flutter.

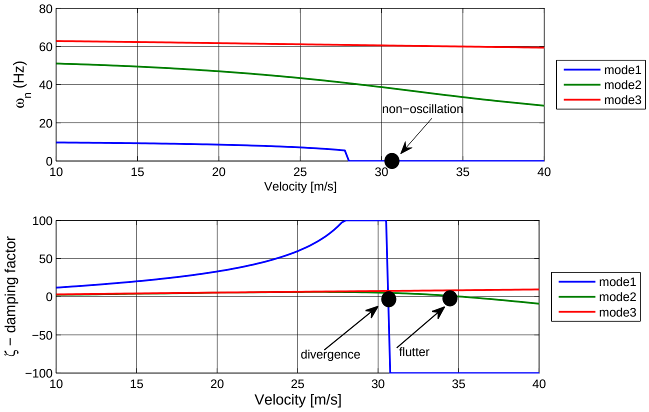

Figure 2: Flutter and Divergence Instabilities

ROBUST OPTIMIZATION

Deb and Gupta (2006) define a robustness as the search to minimize of the objective function $f(x)$, in which the robust solution ($x \in S$, where S is a feasible search space) is obtained when the result presents a small sensitivity to a perturbation around the deterministic values of the decision variables.

There are different approaches devoted to determine robust solution. In this work, the concept of the mean effective objective function proposed by Branke (1998), Tsutsui and Ghosh (1997) and Jin and Sendhoff (2003) is used. Therefore, the associated mathematical problem can be formulated from different forms as follows.

Deb and Gupta (2006) propose the following way to define and find a robust solution to a single-objective optimization problem.

For the minimization of an objective function $f(\mathbf{x})$, a robust solution $\mathbf{x}^*$ is of type I if it is the global minimum of the mean effective function $f^{eff}(\mathbf{x})$ defined with respect to a $\delta-$ neighborhood as follows

$$\textit{Minimize: } f^{eff}(\mathbf{x}) = \frac{1}{|\beta_\delta(\mathbf{x})|} \int_{\mathbf{y}\in\beta_\delta(\mathbf{x})} f(y)dy \tag{22}$$

$$\textit{subject to: } x \in S, \tag{23}$$

Where $\beta_\delta(\mathbf{x})$ is the $\delta-$ neighborhood of solution $\mathbf{x}^*$ and $|\beta_\delta(\mathbf{x})|$ is the hypervolume of the neighborhood.

In this paper it is proposed the following alternative formulation to the optimization problem i:

$$\textit{Minimize: } J = \sum_{1}^{N} \frac{1}{N} \frac{|f^p(x) - f(x)|}{f(x)} \tag{24}$$

$$\textit{subject to: } x \in S, \tag{25}$$

Where $f^p(x)$ is the objective function evaluated for a perturbed set of values of the design variables.

In order to evaluate the objective functions Eq. 22 and Eq. 24, the design variables are sampled by using the Monte Carlo simulation in combination with Latin-Hypercube sampling. In this case, the robust optimization is performed applying uncertainties on tow steering angles of the proposed composite plate model, as show in Fig 3.

The two optimization criteria defined are combined in a multi-objective evolutionary optimization to construct a Pareto front of non-dominant optimal solutions.

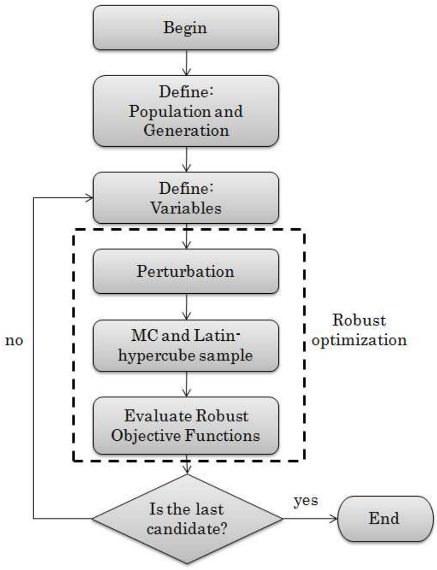

Figure 3: Robust optimization Flowchart

NUMERICAL SIMULATION

A composite wing, previous studied by Hollowell and Dugundji (1984) is idealized as an un-swept rectangular flat plate of chord 76.2mm and semi-span of 305mm fully clamped at its root, as depicted in Fig 4. The plate has six stacked plies of unidirectional graphite/epoxy, the mechanic properties of which are shown in Tab. 1.

A similar model was also been used by Stanford *et al.* (2014), using a the finite element mesh combined with a aerodynamic doublet lattice mesh associated to a finite spline mesh (FPS) used to transfer forces and displacements from the structural module to the aerodynamic model and vice-versa.

It is assumed that the stacking is symmetric and that all the plies have the same entry tow steering angle (T_0) and exit tow steering angle (T_1) (see Eq. 6, which results in only two design variables.

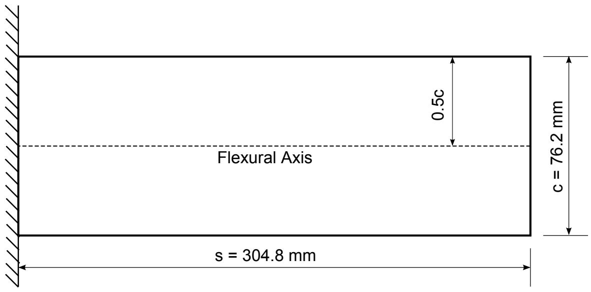

Figure 4: Plate Geometry

Table 1: Material properties and plate dimensions

Property	Value	Property	Value
E_1	98000 Mpa	Span, s	304.8 mm
E_2	7900 Mpa	Chord,c	76.2 mm
G_{12}	5600 Mpa	Density,ρ_0	1520 kg/m^3
μ_{12}	0.28	Ply thickness, t	0.134 mm

Baseline Configurations

Two different symmetric, unsteered configurations, considered as the base, are analyzed. The first configuration (C1) has the stacking sequence of $[0 \quad -45 \quad 45]_s$ and the second configuration (C2) has a different stacking sequence of $[-45 \quad 45 \quad 45]_s$. Figure 5 presents the evolution of the natural frequencies and damping factor associated to the first three modes of the aeroelastic system, computed by solving the eigenvalue problem associated to Eq. (20). It can be seen that flutter instability occurs at flow velocities of 31,0 m/s for C1 and 40,0 m/s for C2.

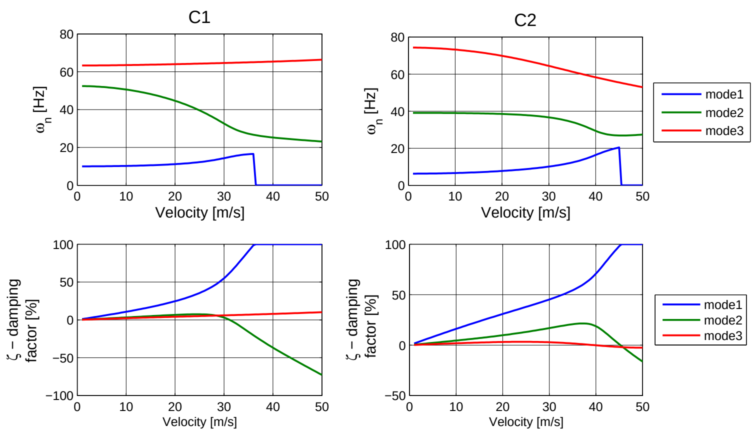

Figure 5: results of aeroelastic analyses for the baseline configurations C1 and C2

Deterministic Optimization

Deterministic optimization was performed aimed at determining the optimal tow steering angles that maximize the lowest flutter and divergence flow speeds. For this purpose, an Evolutionary Algorithm was set with a population of 20 individuals and 20 generations.

It should be made clear that each non-steered stacking sequence is kept for the corresponding steered plate, in the sense that the trajectories followed by the fibers of each ply, according to Fig. 1 and Eq. (6), are rotated according to the orientation of the ply, defined for the non-steered configuration.

Table 2 enables to compare the results of the deterministic optimization with those corresponding to the baseline non-steered configurations. Figure 6 depicts the results of the aeroelastic analyzes of the optimal configurations. It can be seen that optimization provides a 31% increase of the flutter speed for C1, whist this increase is 10% for C2.

Table 2: Results Comparison

non-steered	Flutter Velocity	Steered	Flutter Velocity	Improvement
$[0\ \text{-}45\ 45]_s$	31m/s	T0=-13.84^0 / T1=62.83^0	41m/s	31%
$[\text{-}45\ 45\ 45]_s$	40m/s	T0=-12.0^0 / T1=13.69^0	43.4m/s	9%

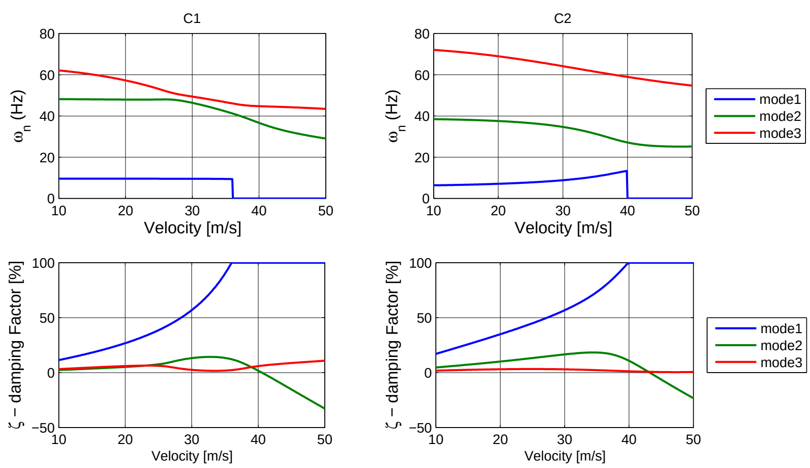

Figure 6: Aeroelastic analysis for optimized configurations

To evaluate the robustness of the optimal solutions, random perturbations, of uniform zero-mean distribution in the range $[-2^0 + 2^0]$ have been introduced in the tow angles. For each sample, the aeroelastic analysis has been performed, as show in Fig. 7. Also indicated are the mean values and variances of the flutter speeds obtained for each configuration. It can be seen that the flutter speeds are quite sensitive to the introduced perturbations.

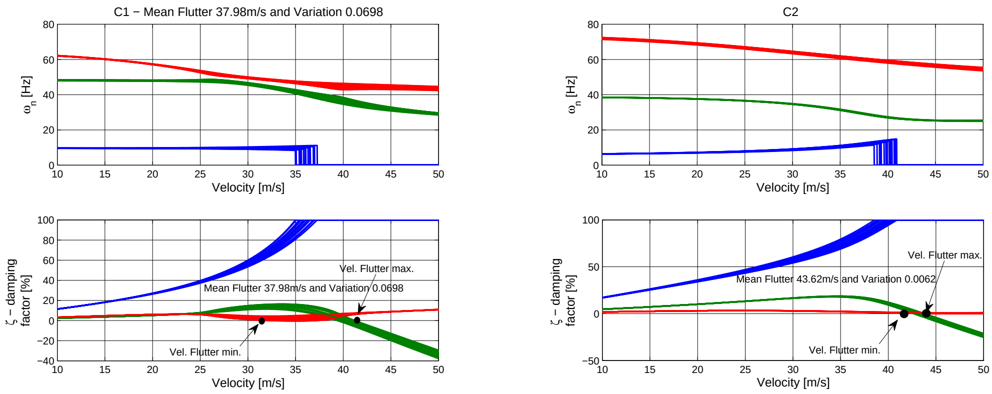

Figure 7: Aeroelastic response of the perturbed optimized configurations

Robust Optimization

To perform robust optimization as previously, random perturbations of maximum amplitudes of ($\pm 2^0$) were introduced in the the tow angle. The robust optimization was carried-out for a six ply symmetric laminate to determine the optimum robust configuration of tow steering angles. The optimization procedure combines a Differential Evolutionary algorithm with a MC simulation coupled with the Latin-Hypercube sampling method. For all optimization runs the population was set with 15 individuals and 15 generations.

As opposed to the previous computations, which were focused on single-objective optimization, hereafter, one considers a multi-objective optimization problem involving, simultaneously, the maximization of mean flutter or divergence velocity (according to Eq. (22)) and the minimization of the variation of flutter/divergence velocity due to the perturbations in the fiber placement angle is (Eq. 24).

The Pareto fronts obtained for the two configurations considered herein are shown in Fig. 8.

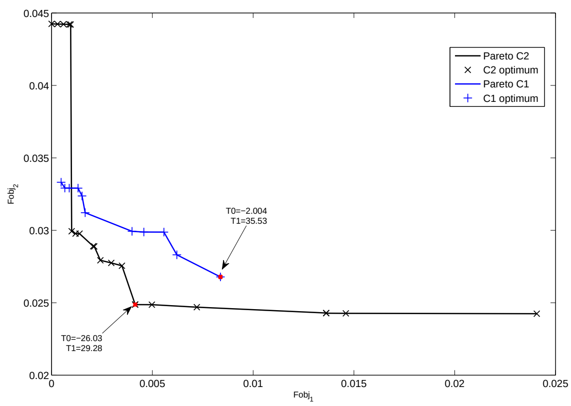

Figure 8: Pareto Front for both configurations

From the ensemble of optimal solutions two have been chosen to evaluate the aeroelastic behavior and robustness with respect to random variations in the tow angle. The results are shown in Fig. 9, where the improvements in terms of both criteria can be clearly noticed. Table 3 provides comparison of the results obtained from deterministic and robust optimizations, subjected to perturbations in tow steering angle. The improvement of robustness in both configurations is evident.

Table 3: Comparison of the results of deterministic and robust optimizations

	Det. Result(C1)	Det. Result(C2)	Rob. Result(C1)	Rob. Result(C2)
T0/T1 ^{0}	-13.84/62.83	-12.0 / 13.69	-2.005 / 35.53	-26.03 / 29.28
Min. Flutter Speed	31.5m/s	42.5m/s	36.42m/s	39.84m/s
Max. Flutter Speed	41.2m/s	43.8m/s	37.86m/s	40.48m/s
Mean. Flutter Speed	37.98m/s	43.26m/s	37.34m/s	40.19m/s
Variation ($fobj_2$)	0.0698	0.0062	0.008378	0.02488

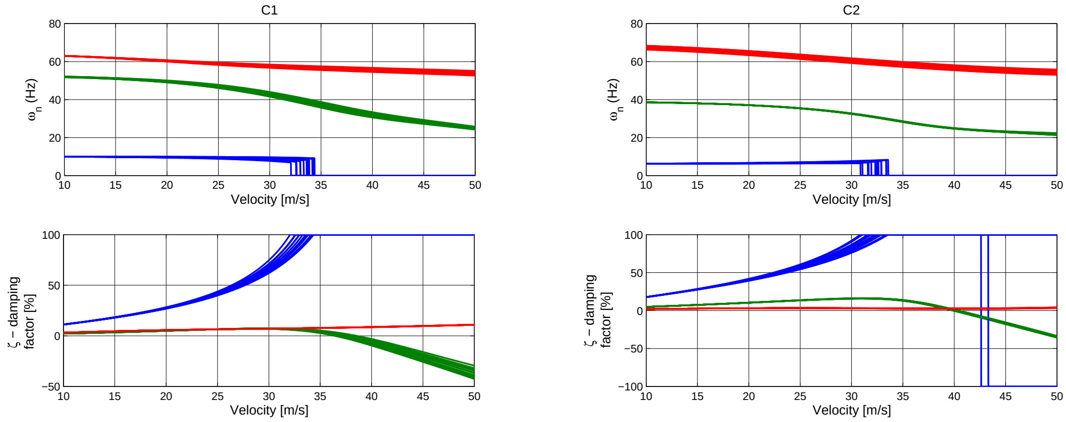

Figure 9: Aeroelastic response for the selected robust solutions

CONCLUSIONS

The deterministic and robust optimization of a simple composite plate was performed on a six-ply symmetric tow steered laminate aiming at increasing aeroelastic stability margins, considering perturbations in the tow place angle of the plies.

The first single-objective optimization runs demonstrated that the deterministic optimization of the tow-steered configurations was capable of increasing the flutter speed. However, the optimal solutions have shown to be quite sensitive to random perturbations in their neighborhood.

Further multi-objective optimization computations integrating a robustness-related criterion provided a set of optimal solutions forming a Pareto front. Solutions extracted from this front demonstrated improved aeroelastic behavior and robustness to perturbations.

Finally, it is important to point-out the importance of evaluating the influence of uncertainties affecting the tow angles of laminate composites and exploring design procedures for minimizing such influence on their structural and aeroelastic behaviors. This aspect is tightly related to the challenge of ensuring the necessary reliability under constraints and imperfections introduced by the manufacturing process.

ACKNOWLEDGMENTS

The authors are thankful to Brazilian Research Agencies CNPQ, CAPES, FAPEMIG, FAPESP and the INCT-EIE for the continuous support to their research work.

REFERENCES

Akhavan, H. and Ribeiro, P., 2011. “Natural modes of vibration of variable stiffness composite laminates with curvilinear fibers”. *Composite Structures*, Vol. 93, No. 11, pp. 3040 – 3047. ISSN 0263-8223. doi:http://dx.doi.org/10.1016/j.compstruct.2011.04.027. URL `http://www.sciencedirect.com/science/article/pii/S0263822311001516`.

Branke, J., 1998. “Creating robust solutions by means of evolutionary algorithms”. In A. Eiben, T. Bäck, M. Schoenauer and H.P. Schwefel, eds., *Parallel Problem Solving from Nature — PPSN V*, Springer Berlin Heidelberg, Vol. 1498 of *Lecture Notes in Computer Science*, pp. 119–128. ISBN 978-3-540-65078-2. doi:10.1007/BFb0056855.

Deb, K. and Gupta, H., 2006. “Introducing robustness in multi-objective optimization”. *Evolutionary Computation*, Vol. 14, No. 4, pp. 463–494.

Gürdal, Z., Tatting, B. and Wu, C., 2008. “Variable stiffness composite panels: Effects of stiffness variation on the in-plane and buckling response”. *Composites Part A: Applied Science and Manufacturing*, Vol. 39, No. 5, pp. 911 – 922. ISSN 1359-835X. doi:http://dx.doi.org/10.1016/j.compositesa.2007.11.015. URL `http://www.sciencedirect.com/science/article/pii/S1359835X07002643`.

Hancock, 1995. *An Introduction to the Flight Dynamics of Rigid Aeroplanes*. Ellis Horwood series in mechanical engineering. Horwood. ISBN 9780133194432.

Hollowell, S.J. and Dugundji, J., 1984. “Aeroelastic flutter and divergence of stiffness coupled, graphite/epoxy cantilevered plates”. *Journal of Aircraft*, Vol. 21, No. 1, pp. 69–76. doi:10.2514/3.48224. URL `http://dx.doi.org/10.2514/3.48224`.

Jin, Y. and Sendhoff, B., 2003. “Trade-off between performance and robustness: An evolutionary multiobjective approach”. In *Evolutionary Multi-Criterion Optimization*, Springer Berlin Heidelberg, Vol. 2632 of *Lecture Notes in Computer Science*, pp. 237–251. ISBN 978-3-540-01869-8. doi:10.1007/3-540-36970-8-17.

Jones, R., 1998. *Mechanics of composite materials*. CRC.

Kim, B.C., Weaver, P.M. and Potter, K., 2014. “Manufacturing characteristics of the continuous tow shearing method for manufacturing of variable angle tow composites”. *Composites Part A: Applied Science and Manufacturing*, Vol. 61, pp. 141–151. ISSN 1359-835X. URL `http://www.sciencedirect.com/science/article/pii/S1359835X14000712`.

Kuo, S.Y. and Shiau, L.C., 2009. “Buckling and vibration of composite laminated plates with variable fiber spacing”. *Composite Structures*, Vol. 90, No. 2, pp. 196 – 200. ISSN 0263-8223. doi:http://dx.doi.org/10.1016/j.compstruct.2009.02.013. URL `http://www.sciencedirect.com/science/article/pii/S0263822309000518`.

Lopes, C., Gürdal, Z. and Camanho, P., 2008. “Variable-stiffness composite panels: Buckling and first-ply failure improvements over straight-fibre laminates”. *Computers and Structures*, Vol. 86, No. 9, pp. 897 – 907. ISSN 0045-7949. doi:http://dx.doi.org/10.1016/j.compstruc.2007.04.016. URL `http://www.sciencedirect.com/science/article/pii/S0045794907001654`. Composites.

Lukaszewicz, D.H.J., Ward, C. and Potter, K.D., 2012. “The engineering aspects of automated prepreg layup: History, present and future”. *Composites Part B: Engineering*, Vol. 43, No. 3, pp. 997–1009. ISSN 1359-8368. URL `http://www.sciencedirect.com/science/article/pii/S1359836811005452`.

Munk, M.M., 1949. “Propeller containing diagonal disposed fibrous material”.

Parnas, L., Oral, S. and Ceyhan, A., 2003. “Optimum design of composite structures with curved fiber courses”. *Composites Science and Technology*, Vol. 63, No. 7, pp. 1071–1082. ISSN 0266-3538. URL `http://www.sciencedirect.com/science/article/pii/S0266353802003123`.

Scarth, C., Sartor, P., Cooper, J.E., Weaver, P. and Silva, G., 2015. “Robust aeroelastic design of a composite wingbox”. In *AIAA SciTech*, American Institute of Aeronautics and Astronautics, pp. –. doi:10.2514/6.2015-0918. URL `http://dx.doi.org/10.2514/6.2015-0918`.

Shirk, M.H., Hertz, T.J. and Weisshaar, T.A., 1986. “Aeroelastic tailoring - theory, practice, and promise”. *Journal of Aircraft*, Vol. 23, No. 1, pp. 6–18. ISSN 0021-8669. doi:10.2514/3.45260.

Stanford, B.K., Jutte, C.V. and Chauncey Wu, K., 2014. “Aeroelastic benefits of tow steering for composite plates”. *Composite Structures*, Vol. 118, pp. 416–422. ISSN 0263-8223. URL `http://www.sciencedirect.com/science/article/pii/S0263822314003973`.

Stodieck, O., Cooper, J.E., Weaver, P. and Kealy, P., 2014. “Optimisation of tow-steered composite wing laminates for aeroelastic tailoring”. In *AIAA SciTech*, American Institute of Aeronautics and Astronautics, pp. –. doi:10.2514/6.2014-0343.

Stodieck, O., Cooper, J.E., Weaver, P.M. and Kealy, P., 2013. “Improved aeroelastic tailoring using tow-steered composites”. *Composite Structures*, Vol. 106, pp. 703–715. ISSN 0263-8223. URL `http://www.sciencedirect.com/science/article/pii/S0263822313003462`.

Tsai, H., 1980. *Introduction to composite materials*. Lancaster: Technomic.

Tsutsui, S. and Ghosh, A., 1997. “Genetic algorithms with a robust solution searching scheme”. *Evolutionary Computation, IEEE Transactions on*, Vol. 1, No. 3, pp. 201–208. ISSN 1089-778X. doi:10.1109/4235.661550.

RESPONSIBILITY NOTICE

The authors are the only responsible for the printed material included in this paper.